AN ANALYTICAL STUDY ON THE ENTROPY GENERATION IN FLOW OF A GENERALIZED NEWTONIAN FLUID

by

Yigit AKSOY[a*], Necmi GURKAN[a], Ayse Bilgen AKSOY[b], Derya DOGAN DURGUN[c], and Ali YURDDAS[a]

[a] Mechanical Engineering, Engineering Faculty, Manisa Celal Bayar University, Manisa, Turkey
[b] Energy Systems Engineering, Technology Faculty, Manisa Celal Bayar University, Manisa, Turkey
[c] Department of Mathematics, Faculty of Science, Manisa Celal Bayar University, Manisa, Turkey

Original scientific paper
https://doi.org/10.2298/TSCI190701360A

In this study, an analytical investigation on pressure driven flow of Powell-Eyring fluid is conducted to understand the irreversibilities due to heat transfer and viscous heating. The flow between infinitely long parallel plates is considered as fully developed and laminar with constant properties and subjected to symmetrical heat fluxes from solid boundaries. The internal heating due to viscous friction accompanies external heat transfer, that is, viscous dissipation term is to be involved in the energy equation. As a cross-check, accuracy of analytical solutions is confirmed by a predictor-corrector numerical scheme with variable step size.

Key words: *generalized Newtonian fluid, heat transfer, entropy generation, perturbation methods.*

Introduction

The early twentieth century, fluid mechanics studies were restricted to the constitutive Newtonian theory that possesses a linear relationship between stress and deformation that lead to constant viscosity. However, exceptional observations of varying viscosity and unusual flow behaviors contradict the theory in consequence of deformation, especially between enough low and very high shear rates. For example, the viscosity deviates from Newtonian behavior, or namely zero shear rate viscosity, as the deformation rate increases up to the infinite shear rate at which it takes constant once again. This transition zone between the limit viscosities typically characterizes the apparent viscosity which decreases or increases within the increasing shear rate. Thus, unlike Newtonian viscosity, apparent viscosity is influenced by the rate of either deformation or shear. Fluids with a decreasing viscosity in response to applied shear rates such as paints, ketchup, and organic liquids are called as shear-thinning, whereas shear-thickening fluids exhibit continuously growing resistance to the flow, for instance, a slurry of corn starch and water mixture. Thanks to emerging of precision and robust instruments, researchers were able to obtain limit viscosities precisely to develop more accurate empirical mathematical models that would be revealed afterward and classified as the generalized Newtonian fluids [1] or GNF for short. It is now essential to clarify that GNF models which capture the only shear thinning and thickening behaviors are not based on either continuum approach or any theoretical molecular insight. Considering the fluid to be mathematically modeled, each GNF model must have

* Corresponding author, e-mail: ygtaksoy@gmail.com

a unique apparent viscosity function and embedded material constants. Thus, the mathematical complexity of a GNF depends on the number of parameters as well as the form of the function fit the flow data. For example, most importantly, through two parameters, The Ostwald–de Waele [2] model in which apparent viscosity varies proportionally to a power-law of shear rate can predict shear thickening and thinning behavior, as well. However, it fails in the prediction of the flow of materials which behave like Newtonian fluid solely in a wide range of low and high shear rates corresponding to constant zero and limit viscosities, respectively. To overcome this situation, more sophisticated fluid models that contain distinct power-law expressions with more than two parameters such as Cross's [3], Carreau's [4] and Carreau-Yasuda's [5] have been proposed to predict the whole shear rate region enclosing limit viscosities as well as the power-law zone.

We previously introduced GNF models as a sub-branch of non-Newtonian fluids in brief. Furthermore, considered GNF is viscous, and besides externally exposed to heat flux. Both heat transfer and the resulting internal heat generation due to viscous dissipation are therefore, not so insignificant as to be negligible, even though material constants do not vary with temperature. Although the word viscous is mostly associated with fluids, viscous dissipation exists in both solid and fluid materials due to the rate of work done for deformation. Since there must be a consistency between a GNF model and Newtonian fluid, it is worth reviewing a few Newtonian studies taking viscous dissipation into account. Considering viscous dissipation as well as wall slip conditions due to rarefaction effects, Kushwaha and Sahu [6] studied a flow throughout parallel plates with various thermal boundary conditions. Aydin and Avci [7] reported a considerable distinction in heat transfer between fluid and considering viscous dissipation; nevertheless, an improvement was observed only for the case where fluid's temperature was higher than solid walls.

On account of design thermally efficient systems, whether fluid parameters are temperature dependent or not, it is quite essential to reconsider obtained mass and heat transfer aspects of performing Second law analysis immediately after ensuring feasibility. While First law of thermodynamics accounts for energy conservation, Second law deals with the irreversibilities, otherwise referred as a reason of deviation from pure thermodynamics ideality, in the system due to various heat transfer mechanisms and viscous dissipation. A proper Second law analysis in flow problems relies on temperature distribution of the fluid to be obtained from the energy balance equationgether with the momentum equation, responsible for velocity distribution. For the rest of the paper, we bring out entropy generation as a result of the Second law analysis with an emphasize on dissipated energy because of viscous dissipation. With this objective in mind, Bejan [8] queried viscous dissipation whether to be negligible in the calculation of entropy generation throughout a few convective heat transfer problems and optimized design configurations of flow geometries to minimize irreversibilities. Accordingly, Hooman [9] reported several studies with inaccurate results, provided that viscous dissipation was not considered. Since GNF models are mathematically comprehensive in nature rather than Newtonian fluids, presentation of analytical expressions, especially those of heat transfer and entropy generation, in closed forms is not an easy task. Sounding studies [10, 11] are therefore, limited to power-law fluids in which mathematical endeavors are relatively simple.

So far, our primary emphasis has been primarily given to the literature on some theoretical basis. Therefore, the intent of this study is to establish a fundamental analytical background of a GNF flow exposed to heat transfer. We have selected the Powell-Eyring model [12, 13] as an operating fluid induced by a constant pressure gradient between parallel plates subjected to symmetric uniform heat flux. Unlike empirical power-law model, with the help of three additional parameters pertaining to the time scale and viscosity constants, Powell-Eyring model can accurately describe, in turn, the transition point from zero shear viscosity to the power-law zone along with infinite shear viscosity. It has a solid theoretical background based on the kinetic theory of fluids, and therefore, can readily make up for shortcomings of the power-law model that has difficulties predicting high concentration solutions and polymer concentrations. It is to be noted; however, the model still has room for progress in terms of heat transfer. To the best of our knowledge, analytical heat transfer terminology is not widely established in comparison with Newtonian and power-law fluid. This untrodden field, therefore, prompted us to study the aspects in the light of the foregoing. We may outline the research to follow a similar path given in [14], in order, as follows; derivation of non-dimensional momentum and energy equations followed by analytical solutions of velocity and temperature profiles, ultimately numerical procedure for validation subsequent to heat transfer aspect and second law analysis.

Definition of the problem and governing equations

Consider the flow of incompressible Powell-Eyring fluid inside infinitely long parallel plates separated by a gap of width $2H$, as illustrated in fig. 1. For convenience, the pressure driven flow is steady and hydrodynamically fully developed since it is far removed from the entrance. For the rest of the analysis, the fluid properties are restricted to constant as well. The fluid is being heated or cooled symmetrically from the impermeable walls with uniform constant heat flux. It should be kept in mind that surfaces are either exposed to constant heat flux or maintained at a constant temperature, but not both.

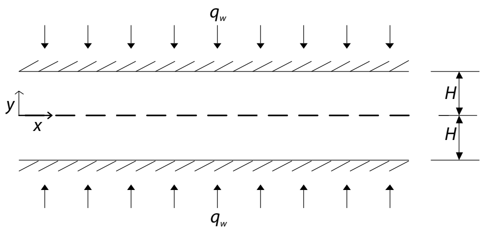

Figure 1. Physical configuration of the problem

Equation of motion: velocity profile

Since our primary concern is velocity profile in the channel, regardless of fluid model, in the absence of body forces, equation of motion in which momentum is conserved along the longitudinal direction in rectangular co-ordinates reduces:

$$\frac{\mathrm{d}}{\mathrm{d}y^*}\tau_{yx} + \frac{\mathrm{d}p}{\mathrm{d}x^*} = 0 \tag{1}$$

where τ_{yx} and $\mathrm{d}p/\mathrm{d}x^*$ are the stress component in direction x^* on plane y^* and negative of pressure gradient, respectively. To proceed further, stress tensor of Powell-Eyring fluid in terms of kinetic variables included in the rate of deformation tensor $\dot{\boldsymbol{\gamma}}$ is defined:

$$\boldsymbol{\tau} = \left[\mu_\infty + \frac{\mu_0 - \mu_\infty}{\lambda|\dot{\gamma}|}\operatorname{arcsin}h\left(\lambda|\dot{\gamma}|\right)\right]\dot{\boldsymbol{\gamma}} \tag{2}$$

where in turn, μ_0, μ_∞, and λ are zero shear viscosity, infinite shear viscosity and time scale parameter [13]. Instead, defining $(\mu_0 - \mu_\infty) / \lambda = 1 / \beta$ and $\lambda = 1 / c$ for ease, the second term in the parenthesis is approximated:

$$\operatorname{arcsin}h\left(\frac{1}{c}|\dot{\gamma}|\right) \approx \frac{|\dot{\gamma}|}{c} - \frac{|\dot{\gamma}|^3}{6c^3} \tag{3}$$

of course, for small deformation rates, *i. e.* $|\dot{\gamma}| \ll 1$. The stress component to be substituted into the momentum equation given in eq. (1) can be readily obtained:

$$\tau_{yx} = \eta \frac{\mathrm{d}u^*}{\mathrm{d}y^*} - \frac{1}{6\beta c_1^3}\left(\frac{\mathrm{d}u^*}{\mathrm{d}y^*}\right)^3 \tag{4}$$

where $\eta = \bar{\mu} + 1 / \beta c_1$ is the modified Newtonian viscosity and u^* is the dimensional velocity in the x^* direction. Now momentum equation:

$$\frac{\mathrm{d}}{\mathrm{d}y^*}\left[\eta \frac{\mathrm{d}u^*}{\mathrm{d}y^*} - \frac{1}{6\beta c_1^3}\left(\frac{\mathrm{d}u^*}{\mathrm{d}y^*}\right)^3\right] + \frac{\mathrm{d}p}{\mathrm{d}x^*} = 0 \tag{5}$$

The boundary conditions of interest:

$$u^*(H) = 0 \,\text{ve}\, \frac{\mathrm{d}u^*}{\mathrm{d}y^*}(0) = 0 \tag{6}$$

that is, no-slip at the upper plate and maximum velocity at the origin due to symmetry. Scaling velocities and lengths with characteristic length, L, and scale velocity, U, the equation of motion along with boundary conditions can be re-written in non-dimensional form:

$$\frac{\mathrm{d}}{\mathrm{d}y}\left[\frac{\mathrm{d}u}{\mathrm{d}y} - \varepsilon\left(\frac{\mathrm{d}u}{\mathrm{d}y}\right)^3\right] + 1 = 0\,, \qquad u(1) = 0 \,\text{and}\, \frac{\mathrm{d}u}{\mathrm{d}y}(0) = 0 \tag{7}$$

in which $\varepsilon = U^2 / (6c^3\eta\beta H^2)$ as a dimensionless Powell-Eyring parameter, and for convenience scale velocity is selected as $U = H^2 / \eta(\mathrm{d}p/\mathrm{d}x^*)$ besides. Applying boundary condition at the origin, it is possible to integrate eq. (7) once. Eventually:

$$\frac{\mathrm{d}u}{\mathrm{d}y} - \varepsilon\left(\frac{\mathrm{d}u}{\mathrm{d}y}\right)^3 = -y \tag{8}$$

In accordance with small parameter assumption, *i. e.*, $\varepsilon \ll 1$, if a regular perturbation expansion is employed in a similar manner given in [15], the velocity distribution varying along is approximated:

$$u = \frac{1}{2}\left(1 - y^2\right) + \frac{\varepsilon}{4}\left(1 - y^4\right) \tag{9}$$

which is identical to the result of [14] for Newtonian fluid, *i. e.*, $\varepsilon = 0$. The essential point here is that the exact solution exists but not practicable to the intents of the study because of its mathematically massive form. Substituting the velocity profile into:

$$u_m = \int_0^1 u \,\mathrm{d}y$$

mean velocity, namely velocity of bulk fluid, is then:

$$u_m = \frac{1}{3} + \frac{\varepsilon}{5} \tag{10}$$

which, again, agrees well with [14] disregarding Powell-Eyring effects. The reader should keep in mind that either velocity profile or mean velocity could be presented in varied forms depending on definition of scale velocity used in the non-dimensionalization.

Equation of energy: temperature profile

Consider the following equation that governs conservation of energy in the steady flow of Powell Eyring fluid according to temperature gradients with viscous dissipation terms:

$$\rho c u^* \frac{\partial T^*}{\partial x^*} = k \frac{\partial T^*}{\partial y^*} + \eta \left(\frac{\mathrm{d}u^*}{\mathrm{d}y^*} \right)^2 - \frac{1}{6\beta c_1^3} \left(\frac{\mathrm{d}u^*}{\mathrm{d}y^*} \right)^4 \tag{11}$$

in which ρ, c, k are the density, specific heat, and thermal conductivity, respectively. Unlike velocity profile, thermally developed temperature profile alters along with x-direction as well as y co-ordinate, *i. e.* $T^* = T^*(x^*, y^*)$. This fact is deduced from the energy equation considering axial conduction term in the left side as given in eq. (11) as well. This term must be retained in the equation as long as isoflux boundary conditions are met, whereas it is not necessary for isothermal walls. However, thermally developed condition states that a non-dimensional temperature profile that is invariant with axial co-ordinate exists under isoflux boundary conditions. Therefore, the axial gradient of the temperature profile and the mean temperature are equal to the same constant, that is [16]:

$$\frac{\partial T^*}{\partial x^*} = \frac{\partial T_m^*}{\partial x^*} = \text{constant} \tag{12}$$

in which

$$T_m^* = \frac{1}{u_m^*} \int_0^1 u^* T^* \mathrm{d}y^* \tag{13}$$

Employing the First law of thermodynamics for the bulk blow reveals axial gradient of the mean temperature as in the following integral form:

$$\frac{\partial T_m^*}{\partial x^*} = \frac{1}{H \rho c u_m^*} \left(q_w'' + \int_0^1 \phi \, \mathrm{d}y^* \right) \tag{14}$$

Designated boundary conditions with respect to symmetrical isoflux walls and maximum temperature at the core:

$$k \frac{\partial T^*}{\partial y^*} \left(x^*, H \right) = q_w'' \text{ and } \frac{\partial T^*}{\partial y^*} \left(x^*, 0 \right) = 0 \tag{15}$$

Despite adequate number of conditions given to solve the second order differential equations, it is not possible to define specific values of both integral constants together because of the conditions just over derivatives. Supplementary condition is the variable wall temperature, *i. e.* $T^*(x^*, H) = T_w^*(x^*)$. Defining $T^* = (T^* - T_w^*) / (Hq_w'')/k$ as a non-dimensional temperature with previous non-dimensional parameters besides, we can reach the following energy equation and boundary conditions in non-dimensional form:

$$\frac{\partial^2 T}{\partial y^2} = \frac{u}{u_m} \left\{ 1 + \mathrm{Br} \int_0^1 \left[\left(\frac{\mathrm{d}u}{\mathrm{d}y} \right)^2 - \varepsilon \left(\frac{\mathrm{d}u}{\mathrm{d}y} \right)^4 \right] \mathrm{d}y \right\} + \mathrm{Br} \left[\varepsilon \left(\frac{\mathrm{d}u}{\mathrm{d}y} \right)^4 - \left(\frac{\mathrm{d}u}{\mathrm{d}u} \right)^2 \right] \tag{16}$$

subjected to $\partial T/\partial y(x,1) = 1$, $\partial T/\partial x(x,0) = 0$ ve $T(x,1)$ where $\mathrm{Br} = \eta U^2/(Hq_w'')$ is the modified Brinkman number. Brinkman number is the ratio between heat production by viscous dissipation inside fluid layers and conducted heat transfer through the fluid exposed by the walls. Substituting the velocity profile obtained in eq. (9) into eq. (16) and retaining the terms up to

$O(\varepsilon)$ in much the same manner as before, however, unlike the momentum equation, performing the direct integration twice along with imposing boundary conditions, temperature profile can be obtained:

$$T=\left(\frac{1}{u_m}+\text{Br}\right)\left(\frac{1}{4}+\frac{\varepsilon}{8}\right)\left(y^2-1\right)+\left[\frac{1}{24}\left(\frac{1}{u_m}+\text{Br}\right)+\frac{\text{Br}}{12}\right]\left(1-y^4\right)+\frac{\varepsilon}{120}\left(\frac{1}{u_m}+5\text{Br}\right)\left(1-y^6\right) \tag{17}$$

Notice that while omission of $O(\varepsilon^2)$ terms, we postulate that u_m in the denominator is of $O(1)$ regardless of ε dependence. Based on following definition of non-dimensional temperature: $T_m = k/(Hq_w)(T_m^* - T_w^*) = -k/(Hh)$ where $q_w'' = h(T_w^* - T_m^*)$, Nusselt number in terms of channel width:

$$\text{Nu}=\frac{2Hh}{k}=\frac{2Hq_w''}{\left(T_w^*-T_m^*\right)k}=-\frac{2}{T_m} \tag{18}$$

In an analytic manner, Nusselt number relative to considered flow of Powell-Eyring fluid is therefore:

$$\text{Nu}=\frac{1386\left(5+3\varepsilon\right)}{1675+909\varepsilon+40\left(5+3\varepsilon\right)^{-1}+\text{Br}\left(297+374\varepsilon\right)} \tag{19}$$

For viscous Newtonian fluid, *i. e.* $\varepsilon = 0$, aforementioned statement turns out to be $\text{Nu} = 70/(17 + 3\text{Br})$ which, although literally true for inviscid flow, *i. e.* $\text{Nu} = 70/17$, is inconsistent with the results for $\text{Br} \neq 0$, such as in [2, 6, 7, 9, 10]. As such, the inconvenience stems from Brinkman number of interests which relies on the characteristic velocity rather than maximum or mean velocity. We hereby invoke Brinkman number in terms of Newtonian mean velocity u_m^* as follows $\overline{\text{Br}} = \eta u_m^{*2}/(\text{W}q_w'')$ where W is the channel width. Substituting $u_m^* = -W/(12\eta)(\text{d}p/\text{d}x^*)$ and $U = (H^2/\eta)(\text{d}p/\text{d}x^*)$ into definitions of Br^* and Br, respectively, as well as $W = 2H$, it is straightforward to figure out $\text{Br} = 18\text{Br}^*$. Recasting eq. (18), refined Nusselt number therefore reads $\text{Nu} = 70/(17 + 54\text{Br}^*)$ which is identical to the result of [9] for $\varepsilon = 0$. Considering Brinkman number $\overline{\text{Br}}$ based on Newtonian maximum velocity, *i. e.* $u_c^* = 3/2$ for the last, Nusselt number, likewise, is re-written as $\text{Nu} = 70/(17 + 24\overline{\text{Br}})$ which, again, is confirmed by [2, 7].

The results presented so far are mainly based on conservation laws of momentum and energy. Vital formulas, especially Nusselt number, to investigate heat transfer mechanisms inside the fluid are obtained. It should be noted that second law analysis is to be considered next in connection with the results in question as well.

Second law analysis

The production of entropy conceptually clarified by the second law of thermodynamics in a system or process is associated with loss of work or waste of useful energy in accordance with Gouy Stodola theorem [17]. Therefore, advanced studies on energy efficiency are aimed specifically at minimizing entropy in thermally efficient systems. In the considered viscous flow, irreversibilities mainly emerge from the heat transfer via conduction as well as the heat generation due to the internal friction. Introducing Peclet number as $\text{Pe} = \rho cHu_m^*/k$ along with $x = x^*/(\text{Pe}H)$ and $\Omega = q_w''H/(kTw)$, the non-dimensional statement of entropy generated in a flow of Powell-Eyring fluid is formed:

$$N=\frac{1}{\text{Pe}^2}\left(\frac{\partial T}{\partial x}\right)^2+\left(\frac{\partial T}{\partial y}\right)^2+\frac{\text{Br}}{\Omega}\left[\left(\frac{\text{d}u}{\text{d}y}\right)^2-\varepsilon\left(\frac{\text{d}u}{\text{d}y}\right)^4\right] \tag{20}$$

which covers heat source irreversibilities due to temperature gradients and viscous heating. Regardless of any point inside the fluid, the mean entropy is defined:

$$\langle N \rangle = \int_0^1 N \, \mathrm{d}y$$

which is, in fact, entropy generation in the bulk fluid. The individual contributions of heat transfer and internal viscous heating to total entropy are observable separately through Bejan number given:

$$\mathrm{Be} = \frac{\dfrac{1}{\mathrm{Pe}^2}\left(\dfrac{\partial T}{\partial x}\right)^2 + \left(\dfrac{\partial T}{\partial y}\right)^2}{\dfrac{1}{\mathrm{Pe}^2}\left(\dfrac{\partial T}{\partial x}\right)^2 + \left(\dfrac{\partial T}{\partial y}\right)^2 + \dfrac{\mathrm{Br}}{\Omega}\left[\left(\dfrac{\mathrm{d}u}{\mathrm{d}y}\right)^2 - \varepsilon\left(\dfrac{\mathrm{d}u}{\mathrm{d}y}\right)^4\right]} \tag{21}$$

correspond to the ratio of those generated by heat transfer to the entire. As seen from the aforementioned statement, while the number of Bejan is reaching the unity, the effect of viscous heating is suppressed, and thus vanishes in overall entropy production. In the interest of brevity as before, mean Bejan number defined:

$$\langle \mathrm{Be} \rangle = \int_0^1 \mathrm{Be} \, \mathrm{d}y$$

is interpreted throughout rest of the paper.

Results and discussion

In this section, the analytical results supported by numerical analysis will be interpreted through figures and tables. Obtaining the first derivative of the velocity the wall from eq. (8), we therefore, treat the system with an IVP solver which is Level 4 and 5 Runge-Kutta-Fehlberg, namely RKF-45 instead of a finite difference scheme.

As shown in fig. 2, the non-Newtonian fluid property is directly proportional to the fluid velocity, and, more clearly, the increase in velocity indicates increasing Powell-Eyring attributes. This observation indicates that flow becomes more uniform over the flow cross-section in much the same manner as shear thinning fluids as long as the constitutive equation assumption defined in eq. (3) prevails. Besides, the analytical solutions based on small parameter assumption inherently diverge from those of numerical as increases.

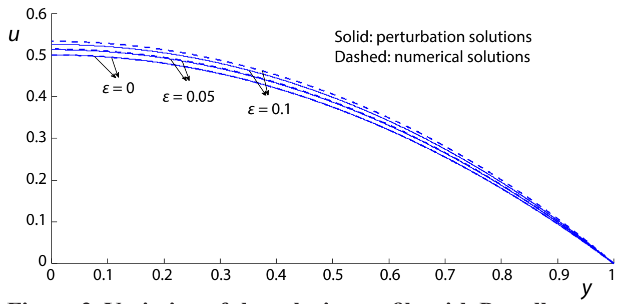

Figure 2. Variation of the velocity profile with Powell-Eyring parameter and numerical comparisons

The temperature of the fluid is apparently insensitive to variation of non-dimensional Powell-Eyring parameter but nevertheless has inconsiderable decrease over its maximum value at the center of the channel as barely shown in fig. 3. This behavior may be similarly related to the fact of temperature decrease as the fluid gets uniformly thinner [10].

A remarkable heat transfer enhancement via mostly convection corresponds to very high Nusselt numbers. Variation of Nusselt number with dimensionless Powell-Eyring parameter and furthermore comparison with numerical results are therefore, visualized in fig. 4 while Brinkman number equals to the unity. From the figure, we simply conclude that Nusselt number to decrease as ε increases, and accordingly convection becomes ineffective compared to the conduction. As another issue in the figure, the Nusselt number predicted in an approximate manner is in almost excellent agreement with the numerical result except for the discrepancies less than 0.1%.

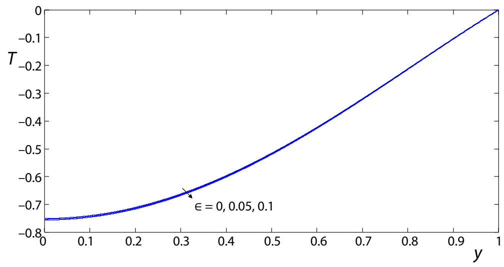

Figure 3. Variation of the temperature with Powell-Eyring parameter (Br = 1)

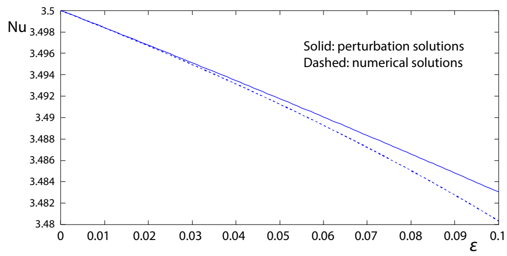

Figure 4. Variation of the Nusselt number with Powell-Eyring parameter and numerical comparisons (Br = 1)

As a conclusion from fig. 5, increasing Brinkman numbers give rise to internal heat production alleviate the external heating, and therefore, induce substantially lower Nusselt numbers. It becomes evident that analytical solutions regarding Nusselt number breaks down while Brinkman number approaching a critical value.

This certain (critical) Brinkman numbers where Nusselt number is non-continuous as a consequence of , as would be expected from eq. (19) which can predict the critical Brinkman number with an error of less than 2.5%, are brought up by fig. 6. It is apparent that the Nusselt number has a different sign around these critical Brinkman numbers since the temperature of bulk fluid approaches either increasingly or decreasingly to the wall temperature for heating or cooling, respectively. Nusselt number fundamentally presents heat transfer rate by convection relative to by conduction and therefore, would be undefined at the critical Brinkman numbers where internal heat production suppresses heat provided by conduction between the walls and the bulk fluid. Also, slightly far from these critical Brinkman numbers, the analytical solution is in excellent agreement with the numerical result as seen from the previous figure.

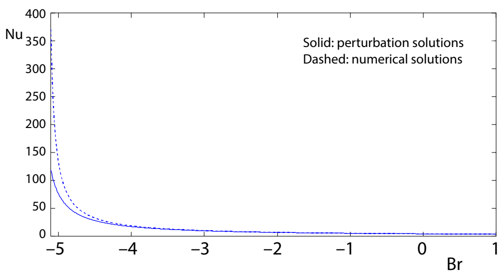

Figure 5. Comparison of perturbation and numerical solutions for the Nusselt number approaching singularity (*ε* = 0.1)

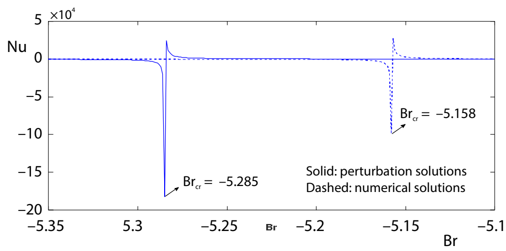

Figure 6. Comparison of perturbation and numerical solutions for a Critical Brinkman number (*ε* = 0.1)

Accuracy of analytical solutions throughout Critical Brinkman numbers corresponding to increasing ε are given in tab. 1. Besides, as Powell-Eyring effects become important, critical Brinkman numbers are shifted towards the infinity.

Table 1. Comparisons of analytical and numerical Critical Brinkman numbers for various Powell-Eyring Parameters

		0	0.02	0.04	0.06	0.08	0.1	0.12
Critical Brinkman number	Analytical	–5.667	–5.586	–5.508	–5.431	–5.357	–5.285	–5.215
	Numerical	–5.667	–5.582	–5.491	–5.392	–5.282	–5.158	–5.011
	% Error	0	0.07	0.31	0.72	1.40	2.40	3.91

To see when irreversibilities emerge considerably and acquire some insight into their nature as well, we here resort to graphs as before. Figure 7 depicts the variation of mean entropy, in other words, aggregate or total entropy, with respect to Brinkman numbers for Newtonian and Powell-Eyring fluids. The optimal Brinkman number gap where total entropy production is relatively weak, and in addition, without any variation related through ε occupies a quite close vicinity of the non-viscous case. Second, beyond this regionwards larger Brinkman numbers, increasing ε values stimulate the entropy generation growth gradually.

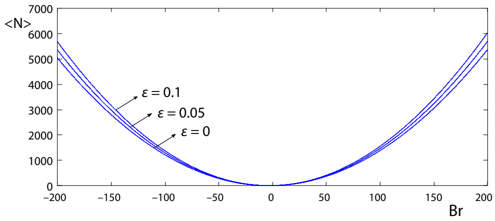

Figure 7. Variation of the mean entropy with Brinkman number for various Powell-Eyring parameters

Since longitudinal heat conduction term is inversely proportional to the square of Peclet number, its contribution immediately vanishes as Peclet number increases and therefore, the mean entropy decreases. When considering a large enough Peclet number, such as order of 10^2, which indicates zero contribution by longitudinal heat conduction, the mean entropy becomes insensitive to the variation of Peclet numbers as numerically tabulated in tab. 2.

Table 2. Comparisons of analytical the mean entropy and Bejan number with numerical solutions at various Peclet numbers for Newtonian and Powell-Eyring fluids

Peclet number	The Mean Entropy				The Mean Bejan Number			
	$\varepsilon = 0$	$\varepsilon = 0.1$			$\varepsilon = 0$	$\varepsilon = 0.1$		
		Analytical	Numerical	%error		Analytical	Numerical	%error
0.1	178.4873	183.8737	185.6462	0.9548	0.9998	0.9998	0.9998	0.0002
1	2.4873	2.5541	2.5758	0.8415	0.9882	0.9879	0.9877	0.0114
10	0.7273	0.7409	0.7451	0.5594	0.9641	0.9630	0.9627	0.0347
100	0.7097	0.7228	0.7268	0.5494	0.9616	0.9604	0.9601	0.0360
1000	0.7095	0.7226	0.7266	0.5493	0.9613	0.9602	0.9599	0.0361

The concept of Bejan number offers us an opportunity of simultaneous consideration of heat transfer and viscous heating over the entropy production. By varying Brinkman number primarily on the horizontal axis and ε secondarily for increasing values as well, variations of Bejan number are plotted in fig. 8. Regardless of ε, the contribution of Brinkman number is, in fact, involved in the total entropy production by both viscous heating directly and temperature gradients indirectly. Reconsidering fig. 8 in view of this fact, in the range of Brinkman number from the zero towards the infinity, Bejan number takes the unity initially, and then, however, exhibits a rapid decrease followed by an inverse peak at a certain Brinkman number. This trend that is apparently insensitive to the variation of ε terminates at the lower extremity when the domination of viscous dissipation over total entropy production expires. Passing a local minimum of Bejan number, curves get to increase with decreasing momentum and subsequently converge to the unity which manifests that the entropy production mainly arises from temperature gradients instead of viscous dissipation. Also, the dependence of ε is easily visible as compared to the left interest of the minimum. We can, therefore, state that as ε increases, Bejan numbers expose slight increments.

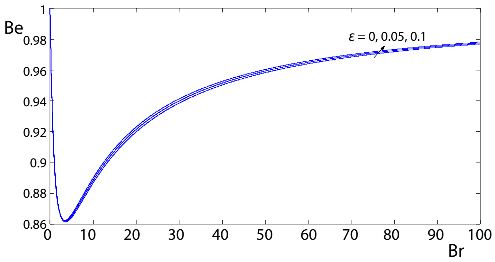

Figure 8. Variation of mean Bejan number with Brinkman number for various Powell-Eyring parameters (Pe = 1, Ω = 10)

Conclusions

Considering a GNF model, the principal objective of this study is to reinforce the concept of non-Newtonian fluids in terms of heat transfer aspects and hereby the Second law of thermodynamics. Newtonian Nusselt number expression peculiar to our flow geometry are extended to Powell-Eyring fluid mode for the first time in the scope of this study.

In sum, the chief results pursuing the lay-out of the study are the following.

- As Powell-Eyring parameter increases, the fluid gains velocity uniformly throughout the cross-section of the channel.
- Maximum temperature occurring at the core due to symmetry decreases in the presence of increasing Powell-Eyring parameter and accordingly a slight decrease in non-dimensional temperature.
- Nusselt number monotonically declines with Powell-Eyring parameter increasing in a short range, *i. e.* $0 < \varepsilon \leq 0.1$.
- Nusselt numbers converge to the infinity at critical Brinkman numbers, whereas, decrease as Brinkman number increase.
- Although entropy production increases with increasing Powell-Eyring parameter, this fact is, indeed, valid for Brinkman numbers sufficiently far from the non-viscous case, *i. e.* Br = 0, otherwise almost no variance.
- As Powell-Eyring parameter increases, Bejan number increases insignificantly, whereas Brinkman number alters Bejan number in a peculiar manner; in other words, Bejan number exhibits a lower extremity between rapid decrease and increase as Brinkman number increase.

Although a comprehensive investigation has been made, further studies can expand the scope into farther GNA models, hydrodynamic and thermal considerations. And besides, more general solution procedures can be constructed as a consequence of revising simplifying assumptions.

References

[1] Morrison, F. A., *Understanding Rheology*, Oxford University Press, New York, USA, 2001
[2] Tso, C. P., *et al.*, Viscous Dissipation Effects of Power-Law Fluid-Flow within Parallel Plates with Constant Heat Fluxes, *Journal Non-Newtonian Fluid Mech.*, *165* (2010), 11-12, pp. 525-630
[3] Galindo-Rosales, F. J., *et al.*, How Dr. Malcom M. Cross May Have Tackled the Development of An Apparent Viscosity Function for Shear Thickening Fluids, *Journal Non-Newtonian Fluid Mech.*, *166* (2011), 23-24, pp. 1421-1424

[4] Georgiou, G. C., The Time-Dependent, Compressible Poiseuille and Extrudate-Swell Flows of a Carreau Fluid with Slip at the Wall, *Journal Non-Newtonian Fluid Mech*., *109* (2003), 2-3, pp. 93-114
[5] Yasuda, K., *et al.*, Shear-Flow Properties of Concentrated Solutions of Linear and Star-Branched Polystyrenes, *Rheol. Acta*, *20* (1981), 2, pp. 163-178
[6] Kushwaha, H. M., Sahu, S. K., Effects of Viscous Dissipation and Rarefaction on Parallel Plates with Constant Heat Flux Boundary Conditions, *Chem. Eng. Technol*., *38* (2015), 2, pp. 1-12
[7] Aydin, O., Avci, M., Viscous-Dissipation Effects on the Heat Transfer in a Poiseuille Flow, *Applied Energy*, *83* (2006), 5, pp. 495-512
[8] Bejan, A., A Study of Entropy Generation in Fundamental Convective Heat Transfer, *Journal Heat Trans*., *101* (1979), 4, pp. 718-725
[9] Hooman, K., Entropy Generation for Microscale Forced Convection: Effects of Different Thermal Boundary Conditions, Velocity Slip, Temperature Jump, Viscous Dissipation, and Duct Geometry, *Int. Commun. Heat Mass*, *34* (2007), 8, pp. 945-957
[10] Shojaeian, M., Kosar, A., Convective Heat Transfer and Entropy Generation Analysis on Newtonian and Non-Newtonian Fluid-Flows between Parallel-Plates under Slip Boundary Conditions, *Int. J. Heat Mass Tran*., *70* (2014), Mar., pp. 664-673
[11] Matin, M. H., Khan, W. A., Entropy Generation Analysis of Heat and Mass Transfer in Mixed Electrokinetically and Pressure Driven Flow through a Slit Micro-Channel, *Energy*, *56* (2013), July, pp. 207-217
[12] Hina, S., *et al.*, Peristaltic Transport of Powell-Eyring Fluid in a Curved Channel with Heat/Mass Transfer and Wall Properties, *Int. J. Heat Mass Tran*., *101* (2016), Oct., pp. 156-155
[13] Yoon, H. K., Ghajar, A. J., A Note on the Powell-Eyring Fluid Model, *Int. Comm. Heat Mass Transfer*, *14* (1987), 4, pp. 381-390
[14] Aksoy, Y., Effects of Couple Stresses on the Heat Transfer and Entropy Generation Rates for a Flow between Parallel Plates with Constant Heat Flux, *Int. J. Therm. Sci*., *107* (2016), Sept., pp. 1-12
[15] Nayfeh, A. H., *Perturbation Methods*, John Wiley and Sons, New York, USA, 2000
[16] Kays, W., *et al.*, *Heat and Mass Transfer*, McGraw-Hill, New York, USA, 2005
[17] Bejan, A., *Entropy Generation Minimization*, CRC Press, Boca Raton, Fla., USA, 1996

Paper submitted: July 1, 2019
Paper revised: August 20, 2019
Paper accepted: August 22, 2019